



Received 27 May 2019
Accepted 5 July 2019

Edited by A. J. Lough, University of Toronto,
Canada

Keywords: crystal structure; 4-methoxyphenyl ring; benzonitrile; face-to-face π – π stacking interactions; Hirshfeld surface analysis.

CCDC reference: 1938782

Supporting information: this article has supporting information at journals.iucr.org/e

Crystal structure and Hirshfeld surface analysis of (*E*)-4-{[2,2-dichloro-1-(4-methoxyphenyl)ethenyl]diazenyl}benzonitrile

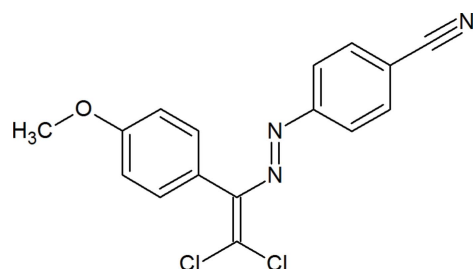
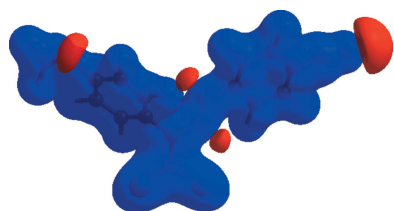
Mehmet Akkurt,^a Namiq Q. Shikaliyev,^b Ulviyya F. Askerova,^b Sevinc H. Mukhtarova,^b Gunay Z. Mammadova^b and Flavien A. A. Toze^{c*}

^aDepartment of Physics, Faculty of Sciences, Erciyes University, 38039 Kayseri, Turkey, ^bOrganic Chemistry Department, Baku State University, Z. Xalilov str. 23, Az, 1148 Baku, Azerbaijan, and ^cDepartment of Chemistry, Faculty of Sciences, University of Douala, PO Box 24157, Douala, Republic of Cameroon. *Correspondence e-mail: toflavien@yahoo.fr

In the title compound, $C_{16}H_{11}Cl_2N_3O$, the 4-methoxy-substituted benzene ring makes a dihedral angle of $41.86(9)^\circ$ with the benzene ring of the benzonitrile group. In the crystal, molecules are linked into layers parallel to (020) by C–H···O contacts and face-to-face π – π stacking interactions [centroid–centroid distances = 3.9116 (14) and 3.9118 (14) Å] between symmetry-related aromatic rings along the *a*-axis direction. A Hirshfeld surface analysis indicates that the most important contributions to the crystal packing are from Cl···H/H···Cl (22.8%), H···H (21.4%), N···H/H···N (16.1%), C···H/H···C (14.7%) and C···C (9.1%) interactions.

1. Chemical context

Weak interactions, such as hydrogen, aerogen, halogen, chalcogen, pnictogen, tetrel and icosagen bonds, as well as *n*– π^* , π – π stacking, π –cation, π –anion and hydrophobic interactions, can control or organize the conformation, aggregation, tertiary and quaternary structure of the molecule, its reactivity, stabilization and other properties (Asadov *et al.*, 2016; Maharramov *et al.*, 2010; Mahmudov *et al.*, 2013, 2014*a,b*, 2015, 2017*a,b*, 2019; Shixaliyev *et al.*, 2013, 2014). The functionalization of azo/hydrazone ligands with non-covalent bond-donor or acceptor sites greatly affects their coordination ability and the catalytic activity of the corresponding coordination compounds (Akbari *et al.*, 2017; Gurbanov *et al.*, 2018; Karmakar *et al.*, 2016; Kopylovich *et al.*, 2011*a,b*; Ma *et al.*, 2017*a,b*; Mahmoudi *et al.*, 2016, 2017*a,b,c*, 2018*a,b,c*). In our previous work, we have attached chloro atoms to dye molecules, which lead to halogen bonding (Atioğlu *et al.*, 2019; Maharramov *et al.*, 2018; Shixaliyev *et al.*, 2018, 2019). In a continuation of this work, we have functionalized a new azo dye, (*E*)-4-{[2,2-dichloro-1-(4-methoxyphenyl)ethenyl]diazenyl}benzonitrile, which provides weak C–H···O intermolecular hydrogen bonds.



OPEN ACCESS

Table 1
Hydrogen-bond geometry (\AA , $^\circ$).

$D-\text{H}\cdots A$	$D-\text{H}$	$\text{H}\cdots A$	$D\cdots A$	$D-\text{H}\cdots A$
$\text{C}2-\text{H}2\cdots \text{O}1^{\text{i}}$	0.95	2.47	3.391 (2)	165
$\text{C}16-\text{H}16\text{C}\cdots \text{O}1^{\text{ii}}$	0.98	2.59	3.516 (3)	158

Symmetry codes: (i) $x - 1, -y + \frac{3}{2}, z + \frac{1}{2}$; (ii) $x - 1, y, z$.

2. Structural commentary

In the title compound, (Fig. 1), the dihedral angle between the 4-methoxy-substituted benzene ring and the benzene ring of the benzonitrile moiety is $41.86(9)^\circ$. The $\text{C}1-\text{C}6-\text{N}1-\text{N}2$, $\text{C}6-\text{N}1-\text{N}2-\text{C}7$, $\text{N}1-\text{N}2-\text{C}7-\text{C}8$, $\text{N}2-\text{C}7-\text{C}8-\text{Cl}1$, $\text{N}2-\text{C}7-\text{C}8-\text{Cl}2$, $\text{Cl}1-\text{C}8-\text{C}7-\text{C}9$ and $\text{C}8-\text{C}7-\text{C}9-\text{C}14$ torsion angles of $24.8(2)$, $-178.37(15)$, $-176.77(17)$, $-2.2(2)$, $178.27(14)$, $-176.26(14)$ and $-52.1(3)^\circ$, respectively, describe the essentially planar conformation of the dichloro-vinyldiazenyl moiety. Bond lengths and angles are within normal ranges and are comparable to those observed in related structures such as (*E*)-1-[2,2-dichloro-1-(4-nitrophenyl)ethenyl]-2-(4-fluorophenyl)diazene (Atioğlu *et al.*, 2019), (*2E*)-1-(2-hydroxy-5-methylphenyl)-3-(4-methoxyphenyl)-prop-2-en-1-one (Fun *et al.*, 2011a), (*2E*)-3-(3-benzyloxyphenyl)-1-(2-hydroxy-5-methylphenyl)prop-2-en-1-one (Fun *et al.*, 2011b), (*2E*)-3-[3-(benzyloxy)phenyl]-1-(2-hydroxyphenyl)prop-2-en-1-one (Fun *et al.*, 2011c), (*2E*)-1-(2,5-dimethoxyphenyl)-3-(3-nitrophenyl)prop-2-en-1-one (Fun *et al.*, 2011d) and (*2E*)-3-(3-nitrophenyl)-1-[4-(piperidin-1-yl)phenyl]prop-2-en-1-one (Fun *et al.*, 2012).

3. Supramolecular features and Hirshfeld surface analysis

In the crystal, the molecules are linked into layers parallel to the (020) plane by $\text{C}-\text{H}\cdots \text{O}$ contacts and face-to-face $\pi-\pi$ stacking interactions [centroid-centroid distances = $3.9116(14)$ and $3.9118(14)$ \AA] along the a -axis between the same aromatic rings (Table 1; Figs. 2 and 3). These molecular layers are held together by weak van der Waals forces.

Hirshfeld surfaces and fingerprint plots were generated for the title compound using *CrystalExplorer* (McKinnon *et al.*, 2007) to quantify and visualize the intermolecular interactions

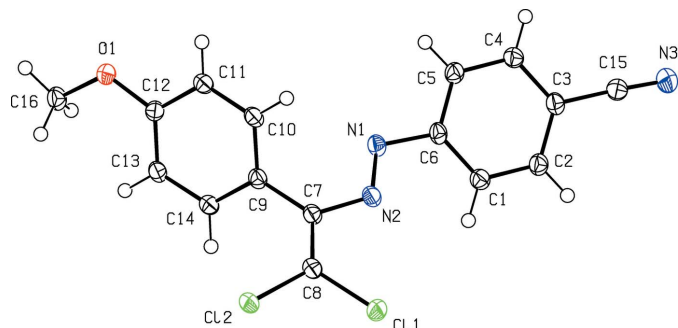


Figure 1

The molecular structure of the title compound, with the atom labelling. Displacement ellipsoids are drawn at the 50% probability level.

Table 2
Summary of short interatomic contacts (\AA) in the title compound.

Contact	Distance	Symmetry operation
$\text{Cl}1\cdots \text{H}5$	3.05	$1+x, \frac{3}{2}-y, \frac{1}{2}+z$
$\text{Cl}1\cdots \text{H}10$	2.98	$x, \frac{3}{2}-y, \frac{1}{2}+z$
$\text{O}1\cdots \text{H}16\text{C}$	2.59	$1+x, y, z$
$\text{Cl}2\cdots \text{N}3$	3.462	$1-x, \frac{1}{2}+y, \frac{3}{2}-z$
$\text{H}16\text{B}\cdots \text{C}13$	2.90	$2-x, 2-y, 1-z$
$\text{O}1\cdots \text{H}2$	2.47	$1+x, \frac{3}{2}-y, -\frac{1}{2}+z$
$\text{H}4\cdots \text{N}3$	2.78	$-x, 1-y, 1-z$
$\text{H}4\cdots \text{N}3$	2.82	$1-x, 1-y, 1-z$
$\text{H}13\cdots \text{H}13$	2.52	$1-x, 2-y, 1-z$

and to explain the observed crystal packing. The Hirshfeld surface mapped over d_{norm} using a standard surface resolution with a fixed colour scale of -0.1603 (red) to 1.2420 (blue) a.u. is shown in Fig. 4. The dark-red spots on the d_{norm} surface arise as a result of short interatomic contacts (Table 2), while the other weaker intermolecular interactions appear as light-red spots. The red points, which represent closer contacts and negative d_{norm} values on the surface, correspond to the $\text{C}-\text{H}\cdots \text{O}$ interactions. The Hirshfeld surface mapped over electrostatic potential (Spackman *et al.*, 2008) is shown in Fig. 5. The red regions indicate atoms with the potential to be hydrogen-bond acceptors (negative electrostatic potential), while blue regions indicate atoms with positive electrostatic

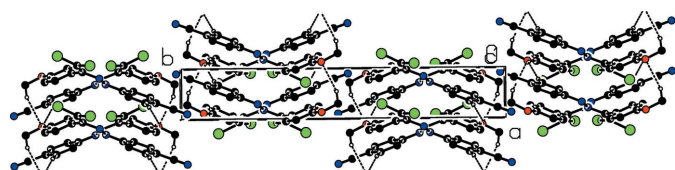


Figure 2

A view of the crystal packing of the title compound. The weak $\text{C}-\text{H}\cdots \text{O}$ interactions are shown as dashed lines and H atoms not involved in hydrogen bonding have been omitted for clarity.

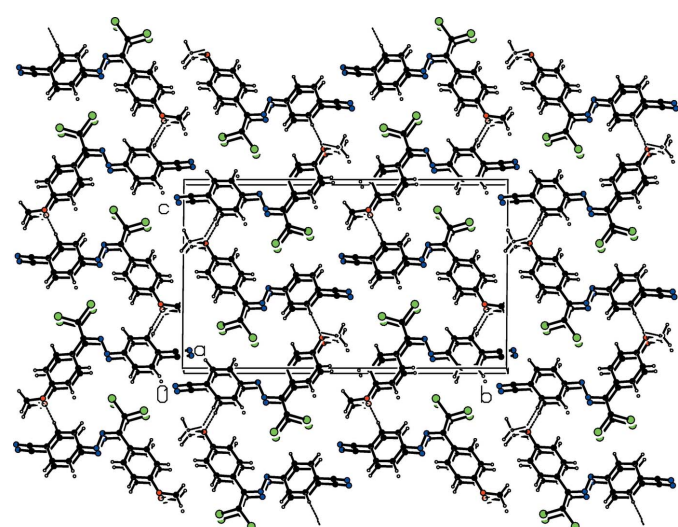


Figure 3

A packing diagram of the title compound, viewed along the a axis. The $\text{C}-\text{H}\cdots \text{O}$ interactions are shown as dashed lines.

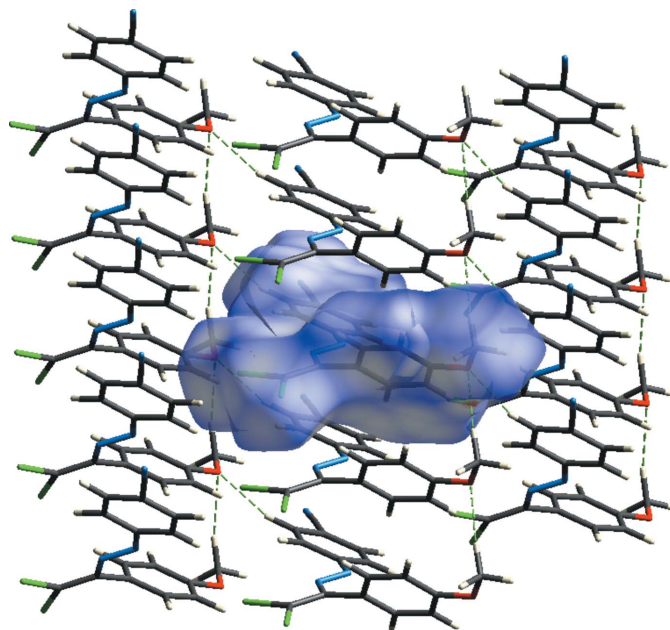


Figure 4

A view of the three-dimensional Hirshfeld surface of the title compound mapped over d_{norm} showing the C–H \cdots O interactions (dashed lines).

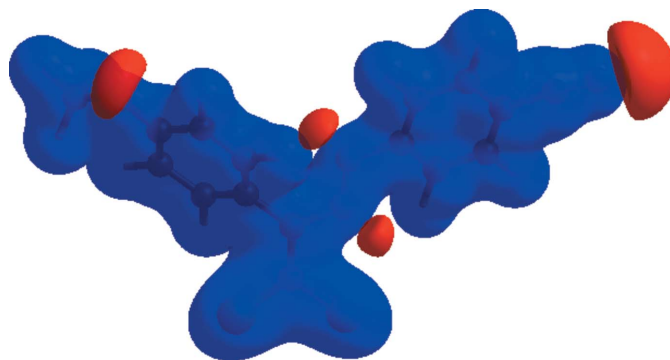


Figure 5

View of the three-dimensional Hirshfeld surface of the title compound plotted over electrostatic potential energy in the range -0.0500 to 0.0500 a.u. using the STO-3 G basis set at the Hartree–Fock level of theory. Hydrogen-bond donors and acceptors are shown as blue and red regions around the atoms, corresponding to positive and negative potentials, respectively.

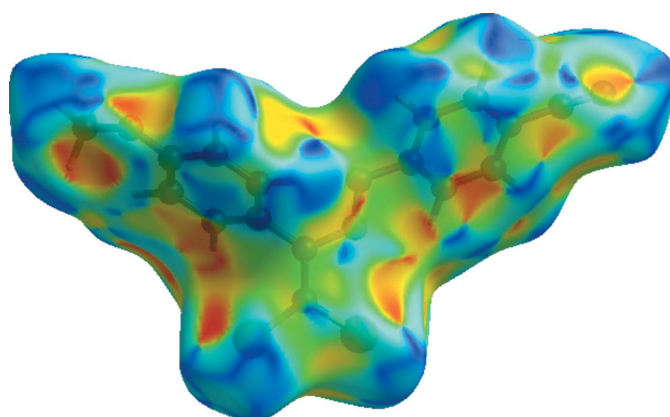


Figure 6
Hirshfeld surface of the title compound plotted over shape-index.

Table 3
Percentage contributions of interatomic contacts to the Hirshfeld surface.

Contact	Percentage contribution
Cl \cdots H/H \cdots Cl	22.8
H \cdots H	21.4
N \cdots H/H \cdots N	16.1
C \cdots H/H \cdots C	14.7
C \cdots C	9.1
O \cdots H/H \cdots O	5.3
N \cdots C/C \cdots N	4.2
Cl \cdots N/N \cdots Cl	2.6
Cl \cdots C/C \cdots Cl	1.7
Cl \cdots Cl	1.6
C \cdots O/O \cdots C	0.4
N \cdots N	0.2

potential, *i.e.* hydrogen-bond donors. The shape-index of the Hirshfeld surface is a tool to visualize the π \cdots π stacking by the presence of adjacent red and blue triangles; if there are no adjacent red and/or blue triangles, then there are no π \cdots π interactions. Fig. 6 clearly suggest that there are π \cdots π interactions in the title compound.

The percentage contributions of the various contacts to the total Hirshfeld surface are shown in the two dimensional fingerprint plots in Table 3. The reciprocal Cl \cdots H/H \cdots Cl interactions appear as two symmetrical broad wings with $d_e + d_i \approx 2.8$ Å and contribute 22.8% to the Hirshfeld surface (Fig. 7b). The H \cdots H interactions appear in the middle of the scattered points in the two dimensional fingerprint plots, with an overall contribution to the Hirshfeld surface of 21.4%

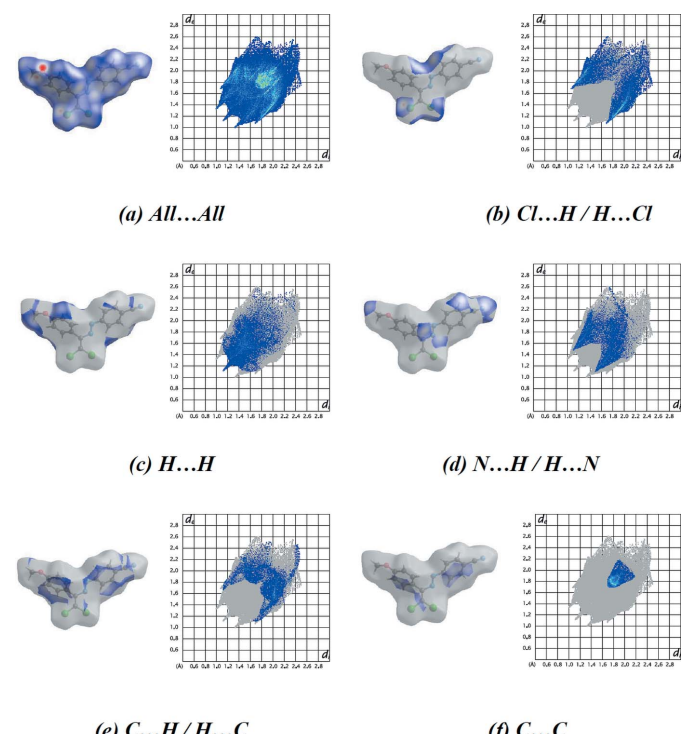


Figure 7
The Hirshfeld surface representations and two-dimensional fingerprint plots of the title compound showing all interactions, and the most significant individual types of interactions.

Table 4
Experimental details.

Crystal data	
Chemical formula	C ₁₆ H ₁₁ Cl ₂ N ₃ O
M _r	332.18
Crystal system, space group	Monoclinic, P2 ₁ /c
Temperature (K)	100
a, b, c (Å)	3.9117 (8), 25.109 (5), 14.968 (3)
β (°)	97.07 (3)
V (Å ³)	1459.0 (5)
Z	4
Radiation type	Synchrotron, λ = 0.80246 Å
μ (mm ⁻¹)	0.63
Crystal size (mm)	0.25 × 0.05 × 0.03
Data collection	
Diffractometer	Rayonix SX165 CCD
Absorption correction	Multi-scan (SCALA; Evans, 2006)
T _{min} , T _{max}	0.850, 0.975
No. of measured, independent and observed [I > 2σ(I)] reflections	22750, 3144, 2978
R _{int}	0.068
(sin θ/λ) _{max} (Å ⁻¹)	0.639
Refinement	
R[F ² > 2σ(F ²)], wR(F ²), S	0.045, 0.123, 1.07
No. of reflections	3144
No. of parameters	201
H-atom treatment	H-atom parameters constrained
Δρ _{max} , Δρ _{min} (e Å ⁻³)	0.30, -0.46

Computer programs: *Marccd* (Doyle, 2011), *iMosflm* (Battye *et al.*, 2011), SHELXLS97 (Sheldrick, 2008), *SHELXL2016* (Sheldrick, 2015), *ORTEP-3* for Windows (Farrugia, 2012) and *PLATON* (Spek, 2009).

(Fig. 7c). The N···H/H···N and C···H/H···C interactions also appear as two symmetrical broad wings with $d_e + d_i \approx 2.6$ and 2.8 Å, respectively, and contribute 16.1 and 14.7%, respectively, to the Hirshfeld surface (Fig. 7d,e). The C···C interactions appear in the middle of the scattered points in the two-dimensional fingerprint plots with an overall contribution to the Hirshfeld surface of 9.1% (Fig. 7f). The small percentage contributions from the other different interatomic contacts to the Hirshfeld surfaces are listed in Table 3. The large number of Cl···H/H···Cl, H···H, N···H/H···N, C···H/H···C and C···C interactions suggest that van der Waals interactions and hydrogen bonding play the major roles in the crystal packing (Hathwar *et al.*, 2015).

4. Synthesis and crystallization

The title compound was synthesized according to the reported method (Atioğlu *et al.*, 2019; Maharramov *et al.*, 2018; Shikhaliev *et al.*, 2018, 2019). A 20 mL screw-neck vial was charged with DMSO (10 mL), (E)-4-[2-(4-methoxybenzylidene)hydrazineyl]benzonitrile (251 mg, 1 mmol), tetramethylethylenediamine (TMEDA; 295 mg, 2.5 mmol), CuCl (2 mg, 0.02 mmol) and CCl₄ (20 mmol, 10 equiv). After 1–3 h (after TLC analysis showed complete consumption of the corresponding Schiff base), the reaction mixture was poured into an 0.01 M solution of HCl (100 mL, pH = 2–3) and extracted with dichloromethane (3×20 mL). The combined organic phase was washed with water (3×50 mL), brine (30 mL), dried over anhydrous Na₂SO₄ and concentrated *in*

vacuo of the rotary evaporator. The residue was purified by column chromatography on silica gel using appropriate mixtures of hexane and dichloromethane (3/1–1/1), giving an orange solid (63%); m.p. 471 K. Analysis calculated for C₁₆H₁₁Cl₂N₃O (M = 332.18): C 57.85, H 3.34, N 12.65; found: C 57.78, H 3.29, N 12.58%. ¹H NMR (300 MHz, CDCl₃) δ 3.83–3.93 (3H, OCH₃), 6.89–7.70 (8H, Ar). ¹³C NMR (75 MHz, CDCl₃) δ 153.89, 133.85, 133.14, 130.54, 130.37, 130.34, 115.49, 115.00, 113.80, 55.51, 29.72, 14.15. ESI-MS: *m/z*: 333.17 [M + H]⁺.

5. Refinement

Crystal data, data collection and structure refinement details are summarized in Table 4. The H atoms of aromatic and methyl groups were placed in calculated positions (C—H = 0.95 and 0.98 Å, respectively) and refined using a riding model with $U_{\text{iso}} = 1.2U_{\text{eq}}$ (C-aromatic) and $1.5U_{\text{eq}}$ (C-methyl).

Funding information

This work was supported by the Science Development Foundation under the President of the Republic of Azerbaijan [grant No. EIF/MQM/Elm-Tehsil-1-2016-1(26)-71/06/4].

References

- Akbari Afkhami, F., Mahmoudi, G., Gurbanov, A. V., Zubkov, F. I., Qu, F., Gupta, A. & Safin, D. A. (2017). *Dalton Trans.* **46**, 14888–14896.
- Asadov, Z. H., Rahimov, R. A., Ahmadova, G. A., Mammadova, K. A. & Gurbanov, A. V. (2016). *J. Surfact. Deterg.* **19**, 145–153.
- Atioğlu, Z., Akkurt, M., Shikhaliev, N. Q., Suleymanova, G. T., Bagirova, K. N. & Toze, F. A. A. (2019). *Acta Cryst. E* **75**, 237–241.
- Battye, T. G. G., Kontogiannis, L., Johnson, O., Powell, H. R. & Leslie, A. G. W. (2011). *Acta Cryst. D* **67**, 271–281.
- Doyle, R. A. (2011). *Marccd software manual*. Rayonix L. L. C., Evanston, IL 60201, USA.
- Evans, P. (2006). *Acta Cryst. D* **62**, 72–82.
- Farrugia, L. J. (2012). *J. Appl. Cryst.* **45**, 849–854.
- Fun, H.-K., Arshad, S., Sarojini, B. K., Khaleel, V. M. & Narayana, B. (2011a). *Acta Cryst. E* **67**, o1248–o1249.
- Fun, H.-K., Arshad, S., Sarojini, B. K., Khaleel, V. M. & Narayana, B. (2011b). *Acta Cryst. E* **67**, o1372–o1373.
- Fun, H.-K., Chia, T. S., Narayana, B., Nayak, P. S. & Sarojini, B. K. (2011d). *Acta Cryst. E* **67**, o3058–o3059.
- Fun, H.-K., Chia, T. S., Nayak, P. S., Narayana, B. & Sarojini, B. K. (2012). *Acta Cryst. E* **68**, o974.
- Fun, H.-K., Loh, W.-S., Sarojini, B. K., Khaleel, V. M. & Narayana, B. (2011c). *Acta Cryst. E* **67**, o1313–o1314.
- Gurbanov, A. V., Maharramov, A. M., Zubkov, F. I., Saifutdinov, A. M. & Guseinov, F. I. (2018). *Aust. J. Chem.* **71**, 190–194.
- Hathwar, V. R., Sist, M., Jørgensen, M. R. V., Mamakhe, A. H., Wang, X., Hoffmann, C. M., Sugimoto, K., Overgaard, J. & Iversen, B. B. (2015). *IUCrJ*, **2**, 563–574.
- Karmakar, A., Paul, A., Mahmudov, K. T., Guedes da Silva, M. F. C. & Pombeiro, A. J. L. (2016). *New J. Chem.* **40**, 1535–1546.
- Kopylovich, M. N., Mahmudov, K. T., Haukka, M., Luzyanin, K. V. & Pombeiro, A. J. L. (2011a). *Inorg. Chim. Acta*, **374**, 175–180.
- Kopylovich, M. N., Mahmudov, K. T., Mizar, A. & Pombeiro, A. J. L. (2011b). *Chem. Commun.* **47**, 7248–7250.

- Ma, Z., Gurbanov, A. V., Maharramov, A. M., Guseinov, F. I., Kopylovich, M. N., Zubkov, F. I., Mahmudov, K. T. & Pombeiro, A. J. L. (2017a). *J. Mol. Catal. A Chem.* **426**, 526–533.
- Ma, Z., Gurbanov, A. V., Sutradhar, M., Kopylovich, M. N., Mahmudov, K. T., Maharramov, A. M., Guseinov, F. I., Zubkov, F. I. & Pombeiro, A. J. L. (2017b). *J. Mol. Catal. A Chem.* **428**, 17–23.
- Maharramov, A. M., Aliyeva, R. A., Aliyev, I. A., Pashaev, F. G., Gasanov, A. G., Azimova, S. I., Askerov, R. K., Kurbanov, A. V. & Mahmudov, K. T. (2010). *Dyes Pigments*, **85**, 1–6.
- Maharramov, A. M., Shikaliyev, N. Q., Suleymanova, G. T., Gurbanov, A. V., Babayeva, G. V., Mammadova, G. Z., Zubkov, F. I., Nenajdenko, V. G., Mahmudov, K. T. & Pombeiro, A. J. L. (2018). *Dyes Pigments*, **159**, 135–141.
- Mahmoudi, G., Bauzá, A., Gurbanov, A. V., Zubkov, F. I., Maniukiewicz, W., Rodríguez-Diéz, A., López-Torres, E. & Frontera, A. (2016). *CrystEngComm*, **18**, 9056–9066.
- Mahmoudi, G., Dey, L., Chowdhury, H., Bauzá, A., Ghosh, B. K., Kirillov, A. M., Seth, S. K., Gurbanov, A. V. & Frontera, A. (2017c). *Inorg. Chim. Acta*, **461**, 192–205.
- Mahmoudi, G., Gurbanov, A. V., Rodríguez-Hermida, S., Carballo, R., Amini, M., Bacchi, A., Mitoraj, M. P., Sagan, F., Kukulka, M. & Safin, D. A. (2017b). *Inorg. Chem.* **56**, 9698–9709.
- Mahmoudi, G., Seth, S. K., Bauzá, A., Zubkov, F. I., Gurbanov, A. V., White, J., Stilinović, V., Doert, T. & Frontera, A. (2018c). *CrystEngComm*, **20**, 2812–2821.
- Mahmoudi, G., Zangrando, E., Mitoraj, M. P., Gurbanov, A. V., Zubkov, F. I., Moosavifar, M., Konyaeva, I. A., Kirillov, A. M. & Safin, D. A. (2018a). *New J. Chem.* **42**, 4959–4971.
- Mahmoudi, G., Zaręba, J. K., Gurbanov, A. V., Bauzá, A., Zubkov, F. I., Kubicki, M., Stilinović, V., Kinzybalo, V. & Frontera, A. (2017a). *Eur. J. Inorg. Chem.* pp. 4763–4772.
- Mahmoudi, G., Zaręba, J. K., Gurbanov, A. V., Bauza, A., Zubkov, F. I., Kubicki, M., Stilinovic?, V., Kinzybalo, V. & Frontera, A. (2018b). *Eur. J. Inorg. Chem.* 4763–4772.
- Mahmudov, K. T., Guedes da Silva, M. F. C., Sutradhar, M., Kopylovich, M. N., Huseynov, F. E., Shamilov, N. T., Voronina, A. A., Buslaeva, T. M. & Pombeiro, A. J. L. (2015). *Dalton Trans.* **44**, 5602–5610.
- Mahmudov, K. T., Gurbanov, A. V., Guseinov, F. I. & Guedes da Silva, M. F. C. (2019). *Coord. Chem. Rev.* **387**, 32–46.
- Mahmudov, K. T., Kopylovich, M. N., Guedes da Silva, M. F. C. & Pombeiro, A. J. L. (2017a). *Dalton Trans.* **46**, 10121–10138.
- Mahmudov, K. T., Kopylovich, M. N., Guedes da Silva, M. F. C. & Pombeiro, A. J. L. (2017b). *Coord. Chem. Rev.* **345**, 54–72.
- Mahmudov, K. T., Kopylovich, M. N., Maharramov, A. M., Kurbanova, M. M., Gurbanov, A. V. & Pombeiro, A. J. L. (2014b). *Coord. Chem. Rev.* **265**, 1–37.
- Mahmudov, K. T., Kopylovich, M. N. & Pombeiro, A. J. L. (2013). *Coord. Chem. Rev.* **257**, 1244–1281.
- McKinnon, J. J., Jayatilaka, D. & Spackman, M. A. (2007). *Chem. Commun.* pp. 3814–3816.
- Sheldrick, G. M. (2008). *Acta Cryst. A* **64**, 112–122.
- Sheldrick, G. M. (2015). *Acta Cryst. C* **71**, 3–8.
- Shikaliyev, N. Q., Ahmadova, N. E., Gurbanov, A. V., Maharramov, A. M., Mammadova, G. Z., Nenajdenko, V. G., Zubkov, F. I., Mahmudov, K. T. & Pombeiro, A. J. L. (2018). *Dyes Pigments*, **150**, 377–381.
- Shikaliyev, N. Q., Çeliksesir, S. T., Akkurt, M., Bagirova, K. N., Suleymanova, G. T. & Toze, F. A. A. (2019). *Acta Cryst. E* **75**, 465–469.
- Shixaliyev, N. Q., Gurbanov, A. V., Maharramov, A. M., Mahmudov, K. T., Kopylovich, M. N., Martins, L. M. D. R. S., Muzalevskiy, V. M., Nenajdenko, V. G. & Pombeiro, A. J. L. (2014). *New J. Chem.* **38**, 4807–4815.
- Shixaliyev, N. Q., Maharramov, A. M., Gurbanov, A. V., Nenajdenko, V. G., Muzalevskiy, V. M., Mahmudov, K. T. & Kopylovich, M. N. (2013). *Catal. Today*, **217**, 76–79.
- Spackman, M. A., McKinnon, J. J. & Jayatilaka, D. (2008). *CrystEngComm*, **10**, 377–388.
- Spek, A. L. (2009). *Acta Cryst. D* **65**, 148–155.

supporting information

Acta Cryst. (2019). E75, 1190-1194 [https://doi.org/10.1107/S2056989019009642]

Crystal structure and Hirshfeld surface analysis of (*E*)-4-{[2,2-dichloro-1-(4-methoxyphenyl)ethenyl]diazenyl}benzonitrile

Mehmet Akkurt, Namiq Q. Shikhaliyev, Ulviyya F. Askerova, Sevinc H. Mukhtarova, Gunay Z. Mammadova and Flavien A. A. Toze

Computing details

Data collection: *Marccd* (Doyle, 2011); cell refinement: *iMosflm* (Battye *et al.*, 2011); data reduction: *iMosflm* (Battye *et al.*, 2011); program(s) used to solve structure: SHELXLS97 (Sheldrick, 2008); program(s) used to refine structure: SHELXL2016 (Sheldrick, 2015); molecular graphics: *ORTEP-3 for Windows* (Farrugia, 2012) and *PLATON* (Spek, 2009); software used to prepare material for publication: *PLATON* (Spek, 2009).

(*E*)-4-{[2,2-Dichloro-1-(4-methoxyphenyl)ethenyl]diazenyl}benzonitrile

Crystal data

C₁₆H₁₁Cl₂N₃O
 $M_r = 332.18$
Monoclinic, $P2_1/c$
 $a = 3.9117$ (8) Å
 $b = 25.109$ (5) Å
 $c = 14.968$ (3) Å
 $\beta = 97.07$ (3)°
 $V = 1459.0$ (5) Å³
 $Z = 4$

$F(000) = 680$
 $D_x = 1.512 \text{ Mg m}^{-3}$
Synchrotron radiation, $\lambda = 0.80246$ Å
Cell parameters from 600 reflections
 $\theta = 1.8\text{--}30.0^\circ$
 $\mu = 0.63 \text{ mm}^{-1}$
 $T = 100$ K
Needle, orange
0.25 × 0.05 × 0.03 mm

Data collection

Rayonix SX165 CCD
diffractometer
/f scan
Absorption correction: multi-scan
(Scala; Evans, 2006)
 $T_{\min} = 0.850$, $T_{\max} = 0.975$
22750 measured reflections

3144 independent reflections
2978 reflections with $I > 2\sigma(I)$
 $R_{\text{int}} = 0.068$
 $\theta_{\max} = 30.9^\circ$, $\theta_{\min} = 1.8^\circ$
 $h = -4 \rightarrow 4$
 $k = -32 \rightarrow 32$
 $l = -19 \rightarrow 19$

Refinement

Refinement on F^2
Least-squares matrix: full
 $R[F^2 > 2\sigma(F^2)] = 0.045$
 $wR(F^2) = 0.123$
 $S = 1.07$
3144 reflections
201 parameters
0 restraints

Hydrogen site location: inferred from
neighbouring sites
H-atom parameters constrained
 $w = 1/[\sigma^2(F_o^2) + (0.066P)^2 + 0.9448P]$
where $P = (F_o^2 + 2F_c^2)/3$
 $(\Delta/\sigma)_{\max} = 0.001$
 $\Delta\rho_{\max} = 0.30 \text{ e } \text{\AA}^{-3}$
 $\Delta\rho_{\min} = -0.46 \text{ e } \text{\AA}^{-3}$

Extinction correction: SHELXL2018
 (Sheldrick, 2015),
 $F_c^* = k F_c [1 + 0.001 x F_c^2 \lambda^3 / \sin(2\theta)]^{-1/4}$
 Extinction coefficient: 0.049 (5)

Special details

Geometry. All esds (except the esd in the dihedral angle between two l.s. planes) are estimated using the full covariance matrix. The cell esds are taken into account individually in the estimation of esds in distances, angles and torsion angles; correlations between esds in cell parameters are only used when they are defined by crystal symmetry. An approximate (isotropic) treatment of cell esds is used for estimating esds involving l.s. planes.

Fractional atomic coordinates and isotropic or equivalent isotropic displacement parameters (\AA^2)

	<i>x</i>	<i>y</i>	<i>z</i>	$U_{\text{iso}}^*/U_{\text{eq}}$
C1	0.4566 (5)	0.66476 (7)	0.67302 (12)	0.0215 (4)
H1	0.463381	0.687885	0.723440	0.026*
C2	0.3294 (5)	0.61359 (7)	0.67752 (13)	0.0221 (4)
H2	0.244963	0.601450	0.730780	0.026*
C3	0.3261 (5)	0.57981 (7)	0.60312 (13)	0.0215 (4)
C4	0.4409 (5)	0.59720 (7)	0.52351 (12)	0.0228 (4)
H4	0.436434	0.574023	0.473208	0.027*
C5	0.5621 (5)	0.64912 (7)	0.51906 (12)	0.0214 (4)
H5	0.636172	0.661965	0.464913	0.026*
C6	0.5748 (5)	0.68213 (7)	0.59378 (12)	0.0197 (4)
C7	0.9517 (5)	0.80678 (7)	0.65882 (12)	0.0199 (4)
C8	1.0851 (5)	0.82299 (7)	0.74254 (13)	0.0218 (4)
C9	0.9344 (5)	0.84019 (7)	0.57700 (12)	0.0199 (4)
C10	1.0545 (5)	0.82125 (7)	0.49838 (13)	0.0210 (4)
H10	1.155098	0.786823	0.498109	0.025*
C11	1.0283 (5)	0.85197 (7)	0.42152 (12)	0.0213 (4)
H11	1.108147	0.838403	0.368576	0.026*
C12	0.8849 (5)	0.90295 (7)	0.42105 (12)	0.0198 (4)
C13	0.7626 (5)	0.92238 (7)	0.49813 (13)	0.0208 (4)
H13	0.662374	0.956840	0.498230	0.025*
C14	0.7886 (5)	0.89082 (7)	0.57518 (13)	0.0210 (4)
H14	0.704725	0.904154	0.627752	0.025*
C15	0.1992 (5)	0.52632 (8)	0.61044 (13)	0.0249 (4)
C16	0.7123 (5)	0.98149 (7)	0.33590 (13)	0.0246 (4)
H16A	0.731494	0.997143	0.276745	0.037*
H16B	0.823240	1.005003	0.383095	0.037*
H16C	0.468596	0.977180	0.343527	0.037*
N1	0.7074 (4)	0.73473 (6)	0.58427 (10)	0.0207 (3)
N2	0.8218 (4)	0.75417 (6)	0.65946 (10)	0.0212 (3)
N3	0.1007 (5)	0.48385 (7)	0.61986 (13)	0.0345 (4)
O1	0.8781 (4)	0.93062 (5)	0.34222 (9)	0.0233 (3)
Cl1	1.07739 (13)	0.78390 (2)	0.83659 (3)	0.02703 (18)
Cl2	1.27416 (13)	0.88356 (2)	0.76669 (3)	0.02496 (18)

Atomic displacement parameters (\AA^2)

	U^{11}	U^{22}	U^{33}	U^{12}	U^{13}	U^{23}
C1	0.0237 (9)	0.0195 (9)	0.0207 (9)	0.0005 (7)	-0.0001 (7)	0.0001 (7)
C2	0.0246 (9)	0.0192 (9)	0.0220 (9)	0.0002 (7)	0.0009 (7)	0.0028 (7)
C3	0.0234 (9)	0.0166 (8)	0.0234 (9)	-0.0005 (7)	-0.0012 (7)	0.0016 (7)
C4	0.0285 (10)	0.0197 (9)	0.0193 (9)	-0.0018 (7)	-0.0009 (7)	-0.0006 (7)
C5	0.0242 (9)	0.0195 (8)	0.0193 (8)	-0.0005 (7)	-0.0021 (7)	0.0024 (7)
C6	0.0207 (9)	0.0154 (8)	0.0218 (9)	0.0007 (7)	-0.0020 (7)	0.0027 (6)
C7	0.0223 (9)	0.0159 (8)	0.0211 (9)	0.0008 (7)	0.0016 (7)	-0.0007 (6)
C8	0.0257 (9)	0.0173 (8)	0.0223 (9)	0.0005 (7)	0.0025 (7)	-0.0010 (7)
C9	0.0215 (9)	0.0167 (8)	0.0207 (9)	-0.0021 (7)	-0.0003 (7)	-0.0006 (6)
C10	0.0244 (9)	0.0159 (8)	0.0221 (9)	0.0002 (7)	0.0000 (7)	-0.0026 (7)
C11	0.0244 (9)	0.0181 (8)	0.0211 (9)	-0.0005 (7)	0.0016 (7)	-0.0021 (7)
C12	0.0221 (9)	0.0186 (8)	0.0179 (8)	-0.0029 (7)	-0.0007 (7)	0.0012 (6)
C13	0.0237 (9)	0.0150 (8)	0.0231 (9)	-0.0004 (7)	0.0006 (7)	-0.0003 (7)
C14	0.0247 (9)	0.0178 (8)	0.0201 (9)	-0.0004 (7)	0.0017 (7)	-0.0018 (6)
C15	0.0294 (10)	0.0231 (10)	0.0217 (9)	-0.0028 (8)	0.0011 (7)	-0.0002 (7)
C16	0.0290 (10)	0.0182 (9)	0.0254 (10)	0.0013 (7)	-0.0015 (7)	0.0030 (7)
N1	0.0225 (8)	0.0161 (7)	0.0227 (8)	0.0004 (6)	-0.0004 (6)	0.0013 (6)
N2	0.0251 (8)	0.0164 (7)	0.0212 (8)	-0.0003 (6)	-0.0007 (6)	-0.0006 (6)
N3	0.0490 (12)	0.0242 (9)	0.0304 (9)	-0.0092 (8)	0.0046 (8)	-0.0008 (7)
O1	0.0307 (7)	0.0186 (6)	0.0203 (7)	0.0020 (5)	0.0018 (5)	0.0023 (5)
Cl1	0.0386 (3)	0.0223 (3)	0.0191 (3)	-0.00365 (18)	-0.00068 (19)	0.00226 (16)
Cl2	0.0343 (3)	0.0185 (3)	0.0213 (3)	-0.00454 (17)	0.00074 (18)	-0.00278 (15)

Geometric parameters (\AA , $^\circ$)

C1—C2	1.382 (3)	C9—C14	1.392 (2)
C1—C6	1.395 (3)	C9—C10	1.403 (3)
C1—H1	0.9500	C10—C11	1.378 (3)
C2—C3	1.399 (3)	C10—H10	0.9500
C2—H2	0.9500	C11—C12	1.397 (3)
C3—C4	1.394 (3)	C11—H11	0.9500
C3—C15	1.441 (3)	C12—O1	1.367 (2)
C4—C5	1.392 (3)	C12—C13	1.391 (3)
C4—H4	0.9500	C13—C14	1.393 (3)
C5—C6	1.388 (3)	C13—H13	0.9500
C5—H5	0.9500	C14—H14	0.9500
C6—N1	1.433 (2)	C15—N3	1.149 (3)
C7—C8	1.359 (3)	C16—O1	1.430 (2)
C7—N2	1.416 (2)	C16—H16A	0.9800
C7—C9	1.479 (2)	C16—H16B	0.9800
C8—Cl2	1.7103 (19)	C16—H16C	0.9800
C8—Cl1	1.7196 (19)	N1—N2	1.257 (2)
C2—C1—C6		C10—C9—C7	121.08 (16)
C2—C1—H1		C11—C10—C9	120.81 (17)

C6—C1—H1	120.3	C11—C10—H10	119.6
C1—C2—C3	119.55 (18)	C9—C10—H10	119.6
C1—C2—H2	120.2	C10—C11—C12	120.36 (17)
C3—C2—H2	120.2	C10—C11—H11	119.8
C4—C3—C2	121.20 (17)	C12—C11—H11	119.8
C4—C3—C15	120.48 (17)	O1—C12—C13	124.46 (17)
C2—C3—C15	118.32 (17)	O1—C12—C11	115.79 (16)
C5—C4—C3	118.80 (17)	C13—C12—C11	119.74 (17)
C5—C4—H4	120.6	C12—C13—C14	119.34 (17)
C3—C4—H4	120.6	C12—C13—H13	120.3
C6—C5—C4	119.96 (17)	C14—C13—H13	120.3
C6—C5—H5	120.0	C9—C14—C13	121.59 (17)
C4—C5—H5	120.0	C9—C14—H14	119.2
C5—C6—C1	121.04 (17)	C13—C14—H14	119.2
C5—C6—N1	116.61 (16)	N3—C15—C3	177.3 (2)
C1—C6—N1	122.33 (16)	O1—C16—H16A	109.5
C8—C7—N2	111.75 (16)	O1—C16—H16B	109.5
C8—C7—C9	124.52 (17)	H16A—C16—H16B	109.5
N2—C7—C9	123.71 (15)	O1—C16—H16C	109.5
C7—C8—Cl2	124.62 (15)	H16A—C16—H16C	109.5
C7—C8—Cl1	122.71 (15)	H16B—C16—H16C	109.5
Cl2—C8—Cl1	112.66 (11)	N2—N1—C6	111.24 (15)
C14—C9—C10	118.16 (17)	N1—N2—C7	116.40 (15)
C14—C9—C7	120.73 (17)	C12—O1—C16	118.13 (15)
C6—C1—C2—C3	0.9 (3)	C14—C9—C10—C11	0.0 (3)
C1—C2—C3—C4	-1.6 (3)	C7—C9—C10—C11	178.04 (17)
C1—C2—C3—C15	178.65 (18)	C9—C10—C11—C12	0.8 (3)
C2—C3—C4—C5	0.3 (3)	C10—C11—C12—O1	178.52 (17)
C15—C3—C4—C5	-179.91 (18)	C10—C11—C12—C13	-1.1 (3)
C3—C4—C5—C6	1.5 (3)	O1—C12—C13—C14	-178.90 (17)
C4—C5—C6—C1	-2.2 (3)	C11—C12—C13—C14	0.7 (3)
C4—C5—C6—N1	179.12 (16)	C10—C9—C14—C13	-0.4 (3)
C2—C1—C6—C5	0.9 (3)	C7—C9—C14—C13	-178.47 (17)
C2—C1—C6—N1	179.54 (17)	C12—C13—C14—C9	0.0 (3)
N2—C7—C8—Cl2	178.27 (14)	C5—C6—N1—N2	-156.50 (17)
C9—C7—C8—Cl2	-3.3 (3)	C1—C6—N1—N2	24.8 (2)
N2—C7—C8—Cl1	-2.2 (2)	C6—N1—N2—C7	-178.37 (15)
C9—C7—C8—Cl1	176.26 (14)	C8—C7—N2—N1	-176.77 (17)
C8—C7—C9—C14	-52.1 (3)	C9—C7—N2—N1	4.8 (3)
N2—C7—C9—C14	126.2 (2)	C13—C12—O1—C16	-4.7 (3)
C8—C7—C9—C10	129.9 (2)	C11—C12—O1—C16	175.67 (16)
N2—C7—C9—C10	-51.9 (3)		

Hydrogen-bond geometry (Å, °)

D—H···A	D—H	H···A	D···A	D—H···A
C2—H2···O1 ⁱ	0.95	2.47	3.391 (2)	165

C16—H16C \cdots O1 ⁱⁱ	0.98	2.59	3.516 (3)	158
------------------------------------	------	------	-----------	-----

Symmetry codes: (i) $x-1, -y+3/2, z+1/2$; (ii) $x-1, y, z$.